*Progress In Electromagnetics Research Letters, Vol. 95, 9–16, 2021*

# An Octaband Temperature Tunable Terahertz Metamaterial Absorber Using Tapered Triangular Structures

**Bhargav Appasani***

**Abstract**—The recent growth of terahertz (THz) applications has sparked interest in the design of novel electromagnetic structures for this frequency regime. One of the structures is the THz absorber, used in sensing and imaging applications. Metamaterial based designs are commonly used to achieve the desired absorption characteristics. Absorbers whose spectra can be tuned by changing the temperature are a subclass in the broad family of THz absorbers that are used for temperature sensing. In the beginning years, single band temperature tunable absorbers were designed, and at present the focus has shifted to the design of multi-band temperature tunable absorbers. Absorbers with six tunable bands have already been proposed. In this paper, an octa-band temperature tunable terahertz metamaterial absorber is proposed, whose unit cell consists of four orthogonally placed tapered triangular structures connected by a ring resonator on top of an InSb dielectric substrate. At 210 K, it is observed that the structure's absorption spectra are: 98.7% at 1.026 THz, 79.5% at 1.245 THz, 90.4% at 1.301 THz, 95.2% at 1.442 THz, 97.44% at 1.585 THz, 96.4% at 1.644 THz, 97.1% at 1.756 THz, and 90.4% at 2.071 THz. The temperature sensitivities of the proposed structure in eight of its absorption bands are 10.3 GHz/K, 8.22 GHz/K, 7.96 GHz/K, 7.02 GHz/K, 6.44 GHz/K, 6.17 GHz/K, 5.5 GHz/K, and 3.2 GHz/K, respectively. Thus, the proposed design can have practical applications in terahertz temperature sensing applications.

## 1. INTRODUCTION

Metamaterials are the latest addition to the field of electromagnetics [1, 2]. The unusual properties displayed by these structures led to their rapid use in various applications ranging from microwave to optical [3–5]. Terahertz (THz) frequency spectrum is in between the microwave and optical frequencies. This frequency spectrum is not yet fully explored, and this void is famously known as the "terahertz gap". However, in the past few decades many novel applications were developed such as terahertz imaging and terahertz sensing. With the growth of these applications research on the design of terahertz metamaterial absorbers (TMAs) has also acquired momentum [6, 7].

A metamaterial absorber is a repeated arrangement of patterns known as unit cells. The periodic arrangement may be 3-dimensional or 2-dimensional. Generally, a TMA is able to absorb the incident THz electromagnetic radiation irrespective of the direction from which it is arriving and its polarization. The first experimental demonstration of a TMA is credited to Yen and his co-researchers [8]. The reason behind the appearance of absorption spectra is the lowering of plasma frequency of the structure [9]. TMAs may display single band or multi-band absorption spectra. Furthermore, these spectra may be tunable or fixed. TMAs whose absorption spectra can be shifted by applying external stimuli such as voltage, mechanical stress, and temperature [10–12] are known as tunable TMAs. Temperature tunable TMAs are those structures whose absorption spectra can be tuned by varying the temperature. These absorbers can be used in temperature sensing applications [13] and for wireless monitoring applications

*Received 15 October 2020, Accepted 21 November 2020, Scheduled 26 November 2020*
* Corresponding author: Bhargav Appasani (appybarkas@gmail.com).
The author is with the School of Electronics Engineering, Kalinga Institute of Industrial Technology, Bhubaneswar, India.

[14]. In the beginning, researchers designed single band temperature tunable TMAs. These structures displayed broad-band absorption characteristics [15, 16]. The tunability of absorption characteristics is a consequence of change in the plasma frequency of the dielectric spacer used in the design of these structures. Usually temperature sensitive material such as InSb is used whose permittivity changes with temperature, thereby resulting in shifting of spectra [17]. Researchers gradually shifted their attention towards increasing the number of absorption bands [18–20]. Recently, a TMA that can offer eight absorption bands has been developed [21]. However, these multi-band TMAs do not display temperature tunability. A six band temperature tunable TMA has been developed that uses an InSb dielectric spacer [19]. In this paper, for the first time an octa band temperature tunable TMA is proposed, whose unit cell consists of four orthogonally placed tapered triangular structures connected by a circular ring on top of an InSb dielectric. It is observed that the structure's absorption spectra at 210 K are: 98.7% at 1.026 THz, 79.5% at 1.245 THz, 90.4% at 1.301 THz, 95.2% at 1.442 THz, 97.44% at 1.585 THz, 96.4% at 1.644 THz, 97.1% at 1.756 THz, and 90.4% at 2.071 THz, while the average temperature sensitivity in eight bands is 6.85 GHz/K. The structure of the unit cell and the physics behind the change in absorption spectra of this structure are described in the second section. The results of the simulation carried out using CST Microwave Studio are reported in the third section. This section also presents the cause of appearance of the different absorption bands using the current distribution plots, and finally, the conclusion is given in the fourth section of the work.

## 2. DESIGN OF THE UNIT CELL

The unit cell structure of the octa-band temperature tunable TMA is depicted in Fig. 1. It has three layers: a bottom ground plane made up of gold and having a thickness of 2 μm, a middle InSb dielectric spacer having a thickness of $h = 16$ μm, and the top 0.4 μm thick gold layer consisting of four orthogonally placed tapered triangular structures connected by a circular ring. The thickness of the bottom layer was taken to be much greater than the skin depth for gold to prevent the transmission of electromagnetic waves. The thickness of the dielectric spacer is optimally taken to achieve maximum absorption in all the bands at different operating temperatures. The conductivity of gold is taken as $4.09 \times 10^7$ S/m. The other dimensions of the structure are $u = 15$ μm and $a = 125$ μm. The four orthogonally placed tapered triangular structures are obtained by cutting four semi-circular rings in a square patch having a side length of $a = 125$ μm. Next, the four triangular structures are connected by a circular ring having an outer radius of 50 μm and an inner radius of 40 μm.

The relative permittivity of the InSb substrate varies with the temperature thereby producing temperature tunable absorption characteristics. The relative permittivity is given by the Drude's model in Equation (1). This equation is applicable when the temperature is between 160 K and 350 K, and

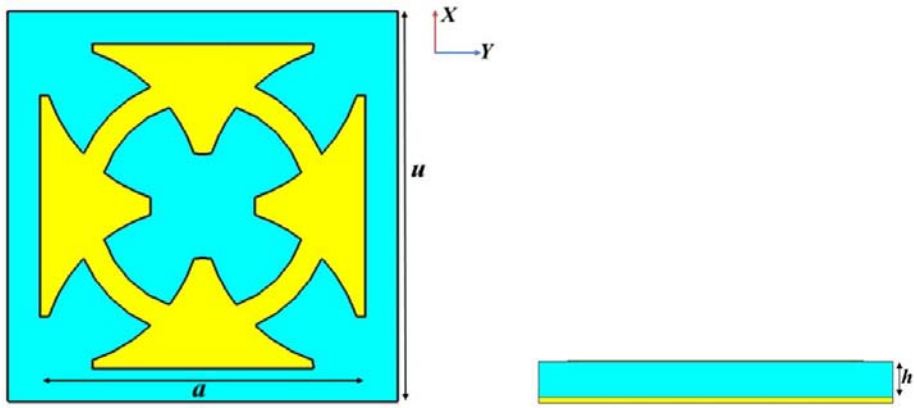


**Figure 1.** Unit cell structure, (a) top view, (b) side view.

the frequency is between 0.1 THz and 2.2 THz [19].

$$\varepsilon_r(\omega) = \varepsilon_\infty - \frac{\omega_P^2}{\omega^2 + j\omega\gamma} \tag{1}$$

where $\omega$ is the frequency of operation in rad/sec, $\omega_P$ the plasma frequency that is given by Equation (2), $\gamma$ the damping constant that is given by Equation (3), and $\varepsilon_\infty$ the permittivity at high frequency. For InSb substrate $\varepsilon_\infty = 15.6$.

$$\omega_P = \sqrt{\frac{Ne^2}{\varepsilon_0 m^*}} \tag{2}$$

$$\gamma = \frac{e}{m^*\mu} \tag{3}$$

where $N$ is the intrinsic density of carriers and is given by Equation (4), $e$ the charge of electron, $\varepsilon_0$ the permittivity of free space, $m^*$ the effective mass of free carriers, and $\mu$ the electron mobility. It has been observed that the electron mobility varies slightly with respect to the temperature between 160 K and 360 K and $m^* = 0.015$ m. As a consequence, the value of $\gamma$ is taken a constant and is $0.1\pi$ THz.

$$N = 5.76 \times 10^{20} T^{1.5} e^{-(0.26/2k_BT)} \tag{4}$$

$k_B$ is the Boltzmann's constant, and $T$ is the temperature in Kelvin. The real and imaginary values of the relative permittivity were obtained using the MATLAB software and are shown in Fig. 2.

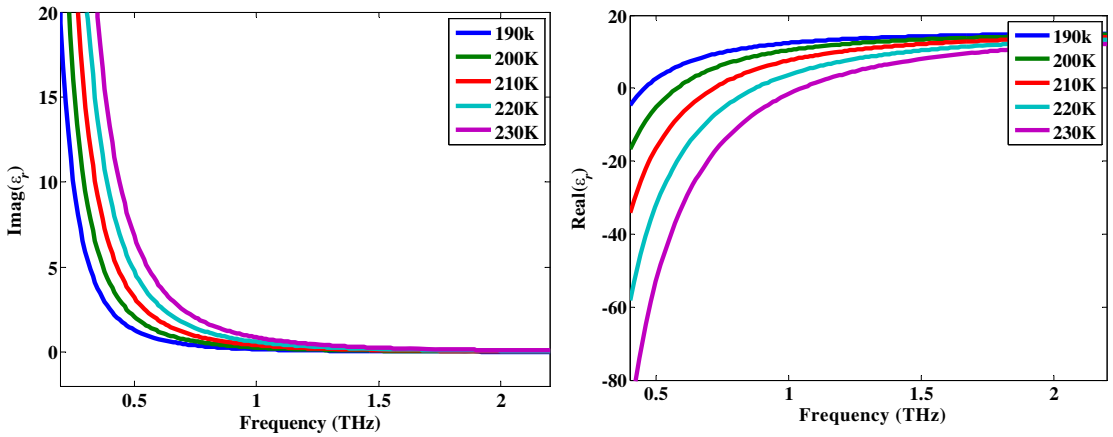


(a) (b)

**Figure 2.** Permittivity of InSb with respect to temperature, (a) imaginary part, (b) real part.

## 3. SIMULATION RESULTS FOR TEMPERATURE TUNABLE SPECTRA

The absorber was designed and simulated using the CST Microwave Studio software. The octa-band absorption characteristics at 210 K are shown in Fig. 3.

The structure has axis symmetry along $x$ axis as well as $y$ axis. Even if the polarization of the incident field is varied, as the structure shows symmetry in the $X$-$Y$ plane, the absorption bands are almost identical. Thus, the design is insensitive to the variations in polarization angle [21]. The absorption bands shift with the temperature, and these characteristics are described in Table 1. The shift in the absorption bands is also illustrated in Fig. 4.

The absorption bands shift towards higher frequency with the increase in temperature. The shift is not uniform in all the bands. Bands at lower frequencies exhibit a greater shift than those at higher frequency. To further understand the shift in the absorption bands, the resonance frequency vs the temperature for each of these bands is plotted in Fig. 5.

**Table 1.** Absorption characteristics at different temperatures.

| | ⟨ Center Frequency (THz), Peak Absorption (%) ⟩ | | | | |
|---|---|---|---|---|---|
| | 190 K | 200 K | 210 K | 220 K | 230 K |
| Band 1 | ⟨0.859, 92.7⟩ | ⟨0.93, 96.97⟩ | ⟨1.026, 98.7⟩ | ⟨1.127, 99.94⟩ | ⟨1.262, 99.84⟩ |
| Band 2 | ⟨1.11, 92.3⟩ | ⟨1.165, 88.24⟩ | ⟨1.25, 79.5⟩ | ⟨1.33, 77⟩ | ⟨1.44, 75.5⟩ |
| Band 3 | ⟨1.163, 95.5⟩ | ⟨1.221, 92.1⟩ | ⟨1.3, 90.4⟩ | ⟨1.37, 86.24⟩ | ⟨1.483, 84⟩ |
| Band 4 | ⟨1.325, 63.6⟩ | ⟨1.37, 78.2⟩ | ⟨1.442, 95.2⟩ | ⟨1.51, 89.8⟩ | ⟨1.61, 97.7⟩ |
| Band 5 | ⟨1.484, 89.8⟩ | ⟨1.525, 92.98⟩ | ⟨1.585, 97.44⟩ | ⟨1.65, 99.21⟩ | ⟨1.743, 99.93⟩ |
| Band 6 | ⟨1.55, 97.3⟩ | ⟨1.588, 96.7⟩ | ⟨1.644, 96.4⟩ | ⟨1.711, 90.4⟩ | ⟨1.797, 89.8⟩ |
| Band 7 | ⟨1.82, 97.3⟩ | ⟨1.854, 97.7⟩ | ⟨1.9, 97.1⟩ | ⟨1.96, 98.6⟩ | ⟨2.04, 98.8⟩ |
| Band 8 | ⟨2.02, 94.7⟩ | ⟨2.052, 93.8⟩ | ⟨2.071, 90.4⟩ | ⟨2.12, 87.8⟩ | ⟨2.18, 52.1⟩ |

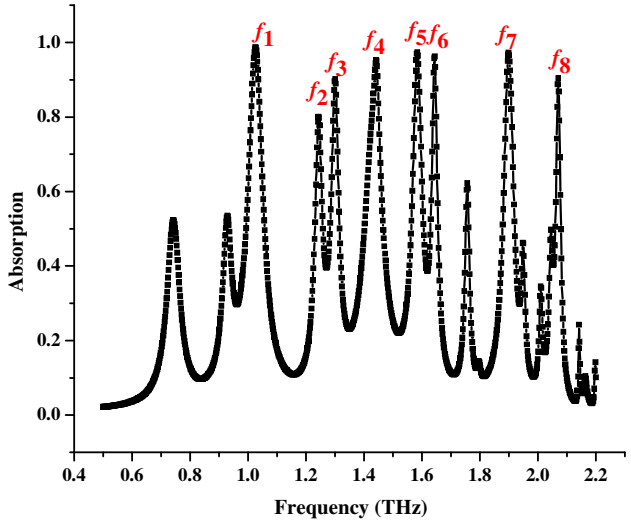


**Figure 3.** Absorption spectra for TE polarization at 210 K.

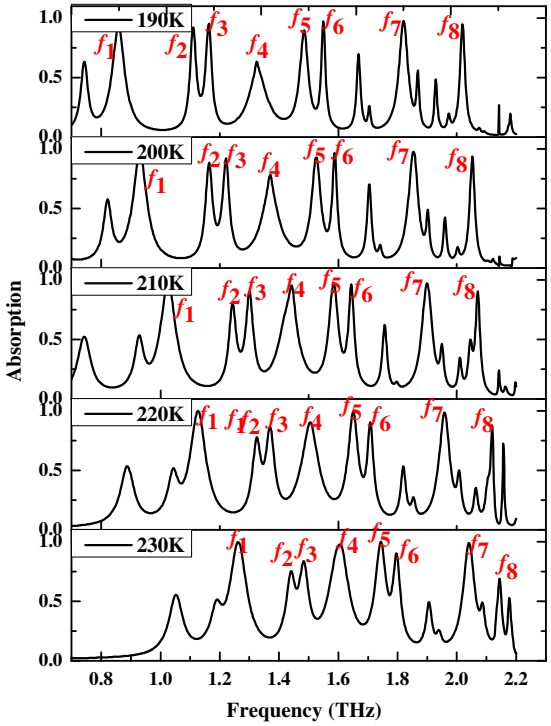


**Figure 4.** The absorption characteristics of the proposed structure at various temperatures.

The temperature sensitivities in the absorption bands are 10.3 GHz/K, 8.22 GHz/K, 7.96 GHz/K, 7.02 GHz/K, 6.44 GHz/K, 6.17 GHz/K, 5.5 GHz/K, and 3.2 GHz/K, respectively. On an average, the structure offers a sensitivity of 6.85 GHz/K. From the absorption characteristics reported in Table 1, it can be observed that six out of the eight absorption bands offer peak absorptions more than 90% at 190 K with the highest absorption of 97.3% at 1.82 THz. At 200 K again six out of eight bands have peak absorptions more than 90%, with the highest absorption of 977% at 1.854 THz. At 210 K, seven out of eight bands offer peak absorptions more than 90% with highest absorption of 98.7% at 1.026 THz. At 220 K and 230 K, four of the eight bands have their peak absorptions greater than 90% with peak absorptions of 99.94% and 99.84% at 1.127 THz and 1.262 THz, respectively. An important feature is that at 230 K, four absorption spectra have peak absorptions greater than 97%. To understand the

absorption mechanism further, the current distributions for different resonance frequencies at 210 K are plotted in Fig. 6.

The current distribution diagrams shown Fig. 6 indicate that the resonance modes are distinct and are not just higher order modes. At 1.026 THz, current distribution is along the tapered triangular structures present along the $x$-axis. In the next absorption mode at 1.25 THz, the current is concentrated along all the edges of the tapering. The absorption mode at 1.3 THz has a similar current distribution due to its close proximity to the absorption mode at 1.25 THz, but the current density is lower. The next resonance mode at 1.442 THz is due to the strong current distribution near the base of the triangular

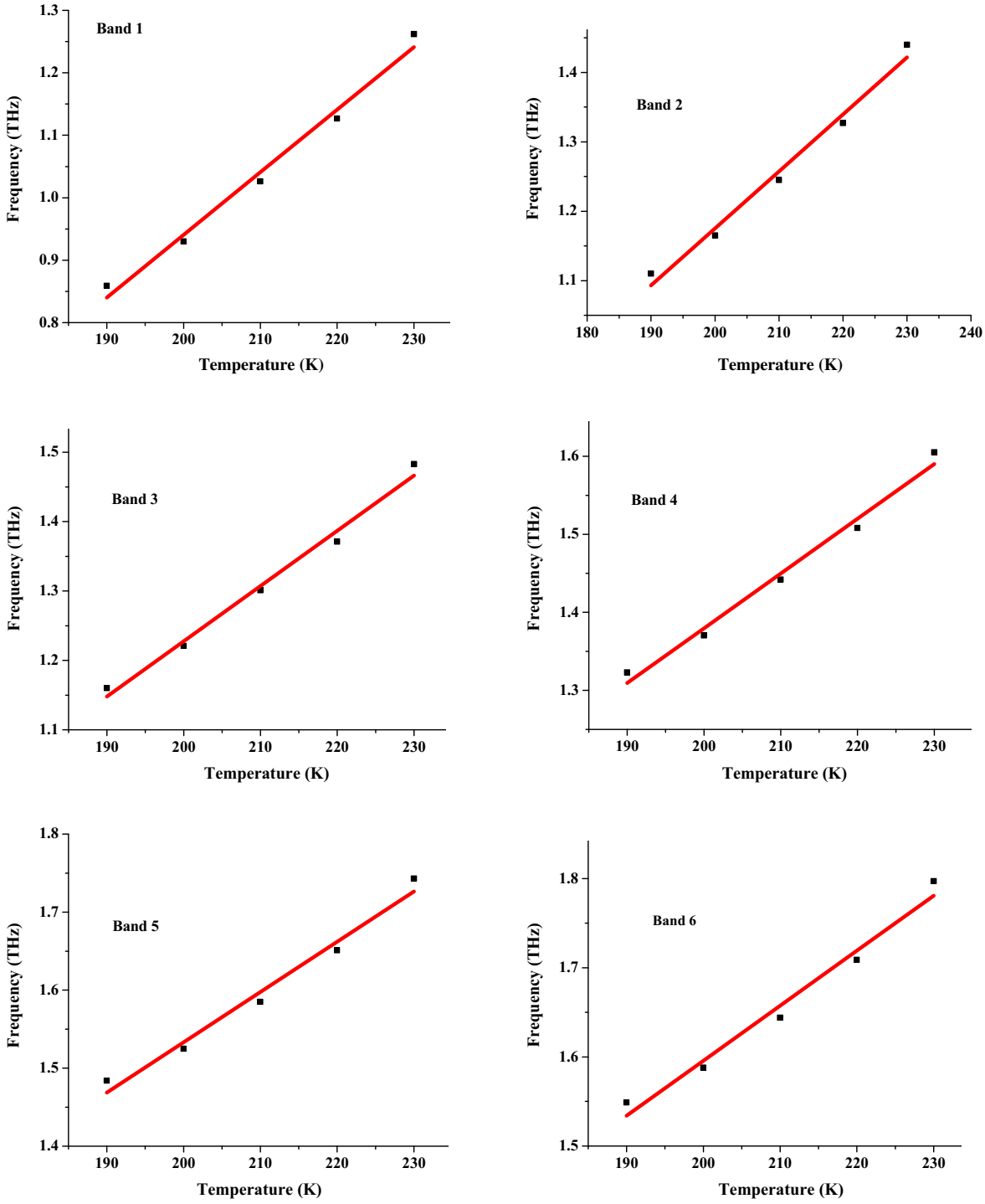

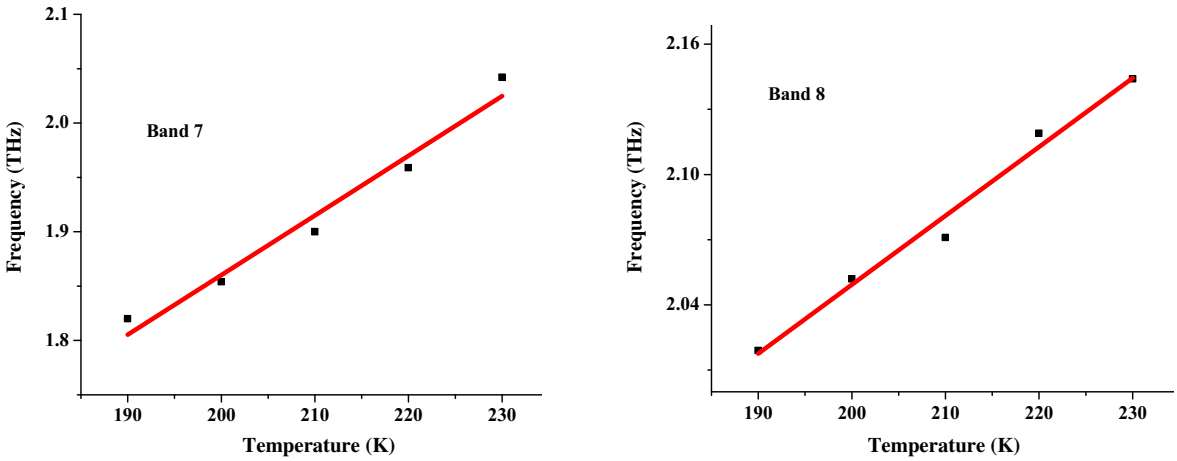


**Figure 5.** Resonant frequency for each band.

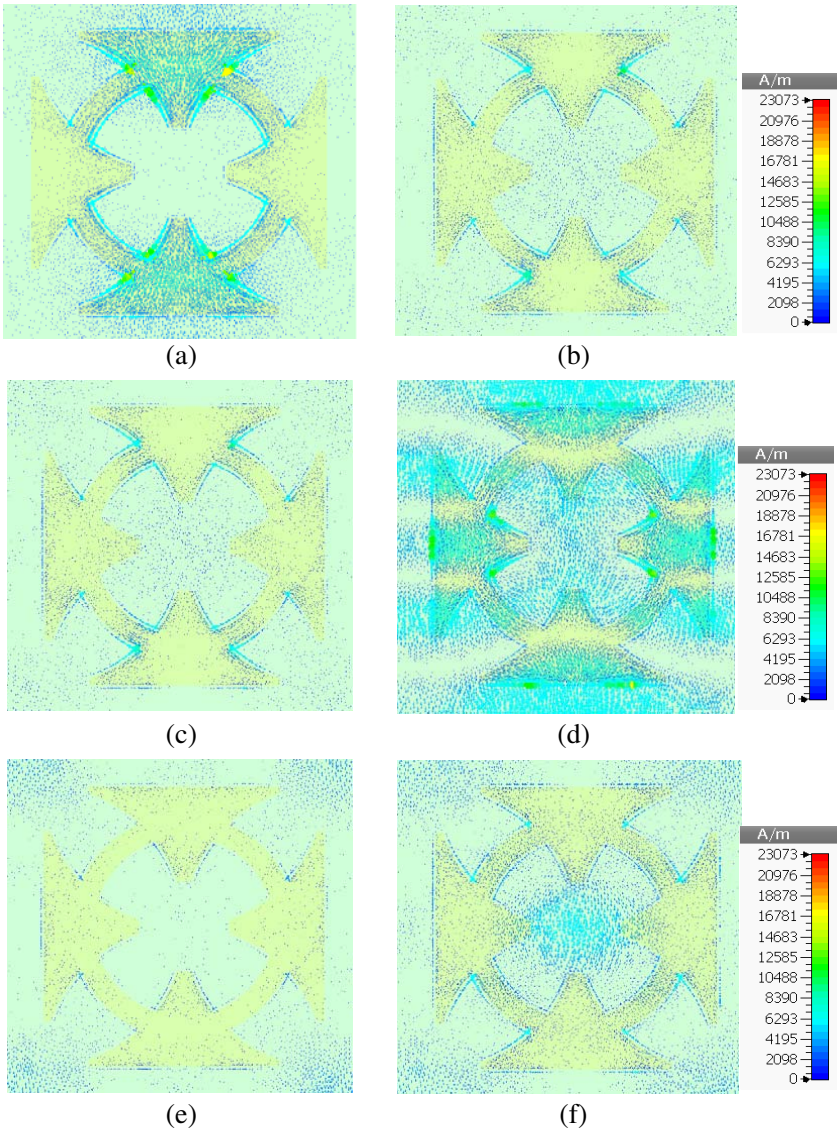

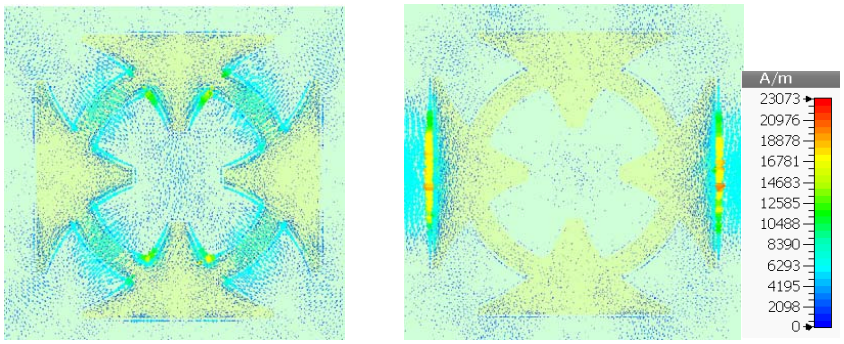


(g) (h)

**Figure 6.** Current distribution at 210 K, (a) 1.026 THz, (b) 1.25 THz, (c) 1.3 THz, (d) 1.442 THz, (e) 1.585 THz, (f) 1.644 THz, (g) 1.9 THz, (h) 2.071 THz.

structures present along $x$-axis and also due to the current distribution at the junction of the tapered structures present along the $y$-axis and the concentric ring. The fifth mode at 1.585 THz has a low current distribution mostly concentrated at the edges of the dielectric. The sixth mode at 1.644 THz has a moderately strong current distribution at the center of the structure. The seventh resonance mode is due to the current distribution along the concentric ring, and the last absorption mode at 2.071 THz is due to the strong current distribution at the base of the triangular structures present along the $y$-axis.

## 4. CONCLUSION

Temperature tunable TMAs can be used for the design of temperature sensors. The tunable characteristics are due to the changes in the plasma frequency of the dielectric. An octa-band temperature tunable TMA is designed, and its characteristics are reported. The design offers a temperature sensitivity of 6.84 GHz/K. Most of these bands have peak absorptions greater than 90%, and at 230 K, four out of the eight bands have absorptions more than 97%. Two of them have near unity absorption. The cause of absorption in the various bands is primarily due to current distributions at the edges of the tapered structures.

## REFERENCES

1. Shamonina, E. and L. Solymar, "Metamaterials: How the subject started," *Metamaterials*, Vol. 1, 12–18, 2007.
2. Veselago, V. G., "The electrodynamics of substances with simultaneously negative values of $\varepsilon$ and $\mu$," *Uspekhi Fizicheskikh Nauk*, Vol. 10, No. 4, 509–514, 1968.
3. Grant, J., I. J. H. Mccrindle, and D. R. S. Cumming, "Multi-spectral materials: Hybridisation of optical plasmonic filters, a mid infrared metamaterial absorber and a terahertz metamaterial absorber," *Optics Express*, Vol. 24, 3451–3463, 2016.
4. Ramakrishna, S. A. and T. M. Grzegorczyk, *Physics and Application of Negative Refractive Index Materials*, CRC Press, Boca Raton, 2008.
5. Landy, N. I., S. Sajuyigbe, J. J. Mock, D. R. Smith, and W. J. Padilla, "Perfect metamaterial absorber," *Physics Review Letters*, Vol. 100, 207402, 2008.
6. Siegel, P. H., "Terahertz technology," *IEEE Transactions on Microwave Theory and Techniques* Vol. 50, No. 3, 910–928, Mar. 2002.
7. Tonouchi, M., "Cutting-edge terahertz technology," *Nature Photonics*, Vol. 1, No. 2, 97–105, 2007.
8. Yen, T. J., et al., "Terahertz magnetic response from artificial materials," *Science*, Vol. 303, 1494–1496, 2004.

9. Rhee, J. Y., Y. J. Yoo, K. W. Kim, Y. J. Kim, and Y. P. Lee, "Metamaterial-based perfect absorbers," *Journal of Electromagnetic Waves and Applications*, Vol. 28, No. 13, 1541–1580, 2014.
10. He, X. Y., X. Zhong, F. T. Lin, and W. Z. Shi, "Investigation of graphene assisted tunable terahertz metamaterials absorber," *Optic Materials Express*, Vol. 6, No. 2, 331–342, 2016.
11. Xiong, H., Q. Ji, T. Bashir, and F. Yang, "Dual-controlled broadband terahertz absorber based on graphene and dirac semimetal," *Optics Express*, Vol. 28, No. 9, 13884–13894, 2020.
12. Hu, F., Y. Qian, Z. Li, J. Niu, et al., "Design of a tunable terahertz narrowband metamaterial absorber based on an electrostatically actuated MEMS cantilever and split ring resonator array," *Journal of Optics*, Vol. 15, No. 5, 055–101, 2013.
13. Wang, B. X., X. Zhai, G. Z. Wang, W. Q. Huang, and L. L. Wang, "Frequency tunable metamaterial absorber at deep-subwavelength scale," *Optic Materials Express*, Vol. 5, 227–235, 2015.
14. Castorina, G., L. Di Donato, A. F. Morabito, T. Isernia, and G. Sorbello, "Analysis and design of a concrete embedded antenna for wireless monitoring applications," *IEEE Antennas and Propagation Magazine*, Vol. 58, No. 6, 76–93, 2016.
15. Wang, B. X. and G. Z. Wang, "Temperature tunable metamaterial absorber at THz frequencies," *Journal of Materials Science: Materials in Electronics*, Vol. 28, No. 12, 1–7, 2017.
16. Song, Z. Y., K. Wang, J. W. Li, and Q. H. Liu, "Broadband tunable terahertz absorber based on vanadium dioxide metamaterials," *Optics Express*, Vol. 26, No. 6, 7148–7154, 2018.
17. Oszwalldowki, M. and M. Zimpel, "Temperature dependence of intrinsic carrier concentration and density of states effective mass of heavy holes in InSb," *Journal of Physics and Chemistry of Solids*, Vol. 49, 1179–1185, 1988.
18. Li, Z. Z., C. Y. Luo, G. Yao, J. Yue, J. Ji, J. Q. Yao, and F. R. Ling, "Design of a concise and dual-band tunable metamaterial absorber," *Chinese Optics Letters*, Vol. 14, No. 10, 102303, 2016.
19. Li, W., D. Kuang, F. Fan, S. Chang, and L. Lin, "Subwavelength B-shaped metallic hole array terahertz filter with InSb bar as thermally tunable structure," *Applied Optics*, Vol. 51, No. 21, 7098–7102, 2012.
20. Zou, H. and Y. Cheng, "Design of a six-band terahertz metamaterial absorber for temperature sensing application," *Optical Materials*, Vol. 88, 674–679, 2019.
21. Verma, V. K., et al., "An octaband polarization insensitive terahertz metamaterial absorber using orthogonal elliptical ring resonators," *Plasmonics*, Vol. 15, No. 1, 75–81, 2020.